

Original Article

Targeting Estrogen Receptor Beta Ameliorates Diminished Ovarian Reserve via Suppression of the FOXO3a/Autophagy Pathway

Fangyuan Li^{1#}, Jingwen Zhu^{1#}, Jinchen Liu², Yongyan Hu³, Peili Wu¹, Cheng Zeng¹, Ruihui Lu¹, Ning Wu¹, Qing Xue^{1*}

¹Department of Obstetrics and Gynecology, Peking University First Hospital, Beijing, China

²Department of Obstetrics and Gynecology, Beijing Tsinghua Changgung Hospital, Beijing, China

³Laboratory Animal Center, Peking University First Hospital, Beijing, China

[Received October 7, 2023; Revised February 19, 2024; Accepted February 21, 2024]

ABSTRACT: Diminished ovarian reserve (DOR) refers to a decrease in the number and/or quality of oocytes, leading to infertility, poor ovarian response and adverse pregnancy outcomes. Currently, the pathogenesis of DOR is largely unknown, and the efficacy of existing therapeutic methods is limited. Therefore, in-depth exploration of the mechanism underlying DOR is highly important for identifying molecular therapeutic targets for DOR. Our study showed that estrogen receptor beta (ER β) mRNA and protein expression was upregulated in granulosa cells (GCs) from patients with DOR and in the ovaries of DOR model mice. Mechanistically, elevated ER β promotes forkhead transcription factor family 3a (FOXO3a) expression, which contributes to autophagic activation in GCs. Activation of FOXO3a/autophagy signalling leads to decreased cell proliferation and increased cell apoptosis and ultimately leads to DOR. In a cyclophosphamide (Cy)-induced DOR mouse model, treatment with PHTPP, a selective ER β antagonist, rescued fertility by restoring normal sex hormone secretion, estrus cycle duration, follicle development, oocyte quality and litter size. Taken together, these findings reveal a pathological mechanism of DOR based on ER β overexpression and identify PHTPP as a potential therapeutic agent for DOR.

Key words: DOR, Estrogen receptor beta, PHTPP, Autophagy, FOXO3a

INTRODUCTION

Diminished ovarian reserve (DOR) usually refers to a decrease in the quality and/or number of oocytes¹. DOR can further develop into premature ovarian insufficiency (POI), which is a primary cause of female infertility². The prevalence of DOR in infertile women is estimated to be between 6% and 64% in different age groups³. DOR is one of the most difficult challenges for assisted reproductive technology (ART) specialists due to the low live birth rate (LBR) and high cancellation rate⁴. The etiology of DOR is thought to be related to genetic, autoimmune, or iatrogenic factors⁵. However, the etiology of DOR has yet to be fully elucidated. Thus, it is

important to investigate the pathogenesis of DOR to identify therapeutic molecular targets for DOR and POI.

DOR is a reproductive system disease caused by a decrease in the quality and quantity of oocytes. Gap junctions are present between granulosa cells (GCs) and oocytes, which facilitate communication between them. The estrogen receptors are mainly expressed on GCs and not on oocytes. Therefore, GCs rely on these receptors to regulate oocyte development and maturation more effectively⁶. Accumulating evidence has confirmed that follicular atresia is triggered by GC apoptosis⁷⁻⁹, and a previous study reported that the GC apoptosis rate was significantly increased in patients with DOR¹⁰. In addition to apoptosis, autophagy has been shown to be involved in follicular loss¹¹. Autophagy is a self-

*Correspondence should be addressed to: Dr. Qing Xue, Department of Obstetrics and Gynecology, Peking University First Hospital, Beijing, China. Email: drxueqing@163.com. # These authors contributed equally to this work.

Copyright: © 2024 Li F. et al. This is an open-access article distributed under the terms of the [Creative Commons Attribution License](https://creativecommons.org/licenses/by/4.0/), which permits unrestricted use, distribution, and reproduction in any medium, provided the original author and source are credited.

degradation process responsible for the disassembly of damaged cell components and recycling of bioenergetic molecules and depends on lysosomes¹². The formation of autophagosomes involves a variety of proteins and complexes and is also regulated by a variety of genes. Autophagy-related genes (ATGs) and Beclin1 are important regulatory genes involved in autophagosome maturation. LC3 is a key structural protein of autophagosomes, and the expression of ATG7, BECLIN1 and LC3 can reflect autophagic activity to a certain extent¹³. Increased autophagic signalling during follicular atresia was observed in rat GCs¹⁴. Recent studies have shown that autophagy is involved in regulating GC apoptosis and accelerating follicular atresia^{15, 16}. This evidence highlights the importance of GC death in the pathogenesis of DOR. However, the underlying mechanism of GC death in DOR remains to be determined.

FOXO3a is a member of the forkhead transcription factor (FOXO) family and plays an important role in the cell cycle, apoptosis, DNA damage repair, oxidative stress, and autophagy¹⁷. Studies have reported that FOXO3a can activate autophagy by regulating the expression of autophagy-regulating genes^{18, 19}. FOXO3a can detect and correct autophagic flux dysfunction, ensuring that cells lacking autophagic capacity undergo apoptotic death²⁰. Furthermore, many studies have shown that FOXO3a is also associated with follicular development. Some researchers have suggested that the FOXO3 protein regulates follicle growth and atresia by promoting apoptosis in mammalian ovarian GCs and oocytes^{13, 21, 22}. However, the relationship between FOXO3a and autophagy in ovarian reserve function needs to be further explored.

Estrogen plays an important role in follicular development²³. There are two subtypes of estrogen receptor (ER), estrogen receptor alpha and beta (ER α and ER β), which are encoded by the estrogen receptor 1 (ESR1) and 2 (ESR2) genes, respectively. Among them, ER β is the main ER subtype in the ovary²⁴ and is abundantly expressed in GCs²⁵, but there is no consensus on the role of ER β in GCs or follicle development. The autophagy-inducing function of ER β has been demonstrated in several cell types, such as breast cancer cells, human seminoma cells, and osteosarcoma cells²⁶⁻²⁹. Moreover, in prostate cancer, ER β causes apoptosis by transactivating FOXO3a³⁰. Currently, there are no consistent findings related to the effects of ER β on oocytes and GCs in follicles, and additional research is needed to confirm whether ER β affects female fertility. However, the relationships between ER β and FOXO3a and between ER β and autophagy in GCs have not been determined, and the effects of ER β on ovarian reserve and female fertility still need to be explored.

Here, we found that overexpression of ER β activated apoptosis through the FOXO3a/autophagy signalling pathway in GCs and ultimately led to DOR. Subsequently, in a DOR mouse model, the ER β antagonist PHTPP was shown to reverse the pathogenesis of DOR, restore the number and quality of oocytes, promote embryonic development, and increase the LBR. The above study provides an experimental basis for ER β as a possible molecular marker and a therapeutic target for DOR.

MATERIALS AND METHODS

Clinical samples

The study was approved by the Institutional Review Board of Peking University (No. 2020 [184]), and informed consent was signed by all participants. Twenty-three women with DOR who received in vitro fertilization or intracytoplasmic sperm injection and embryo transfer (IVF/ICSI-ET) at Peking University First Hospital were included. The diagnostic criteria for DOR were (i) age <40 years, (ii) anti-Müllerian hormone (AMH) level <1.1 ng/mL, and (iii) an ovarian antral follicle count (AFC) <6. Women with a history of ovarian surgery, radiotherapy, chemotherapy, or known chromosomal abnormalities were excluded. Twenty-three women seeking infertility treatment due to male factors or tubal obstruction were enrolled as controls. The inclusion criteria were as follows: i) age <40 years, (ii) 1.4 ng/mL <AMH <4 ng/mL, (iii) 6 ≤ AFC <15, and (iv) basal serum follicle-stimulating hormone (FSH) ≥10 IU/l. The inclusion criteria were based on Chinese expert consensus on the clinical diagnosis and treatment of early-onset ovarian insufficiency in 2017 and the Bologna standard. The clinical characteristics of the participants are summarized in Table 1.

GC isolation

Follicular aspirates obtained from each participant during oocyte retrieval were centrifuged at 3000 rpm at 4°C for 10 minutes, after which the supernatant was removed. Then, phosphate-buffered saline (PBS) was added, and the samples were gently mixed and centrifuged at 4°C and 3000 rpm for 10 min. The precipitates containing human ovarian GCs were washed with PBS once and then resuspended in 1 mL of PBS. Afterwards, 2 mL of Percoll solution was added to the mixture, and the mixture was centrifuged at 4°C and 2000 rpm for 30 min. Next, the second layer of liquid with GCs was transferred to a new centrifuge tube. After gentle mixing with PBS, the mixture was centrifuged at 3000 rpm for 10 min to collect the GCs. Finally, the isolated GCs were snap frozen and stored at -80°C until use.

Table 1. Baseline characteristics in the DOR and control groups.

Variable	Control	DOR	t/ χ^2	P
Embryo transfer cycles (n)	23	23		
Age (years)	33.3 \pm 3.0	35.0 \pm 3.3	-1.883	0.339
Duration of infertility (years)	3.5 \pm 2.4	3.1 \pm 2.0	0.696	0.633
BMI (kg/m ²)	21.4 \pm 2.4	21.7 \pm 3.7	0.681	0.222
Primary infertility rate (%)	17(73.9)	16(69.6)	0.107	0.743
AMH (ng/mL)	2.6 \pm 0.9	0.5 \pm 0.3	11.248	<0.001
Basal FSH (U/L)	7.4 \pm 1.6	13.2 \pm 9.9	-2.783	0.001
Basal LH (U/L)	4.0 \pm 1.6	6.5 \pm 5.9	-1.971	0.011
Basal E2 (pmol/L)	42.3 \pm 21.9	54.8 \pm 59.7	-0.943	0.112
Basal FSH/LH	2.5 \pm 1.5	2.7 \pm 1.9	-0.373	0.922
AFC (n, bilateral)	11.1 \pm 3.4	4.0 \pm 1.9	8.873	0.002
Number of oocytes retrieved(n)	10.2 \pm 5.0	2.5 \pm 2.1	6.788	0.001

BMI, body mass index; AMH, anti-Müllerian hormone; AFC, antral follicular count; E2, oestradiol; FSH, follicle-stimulating hormone

Cell culture

The human ovarian GC line KGN was generously donated by Dr. Jie Qiao of Peking University Third Hospital, Beijing, China, in 2019. KGN cells were cultured in DMEM/F12 supplemented with 1% penicillin–streptomycin and 10% foetal bovine serum in a humidified atmosphere of 5% CO₂ at 37°C.

Transient cell transfection

On the day before transfection, KGN cells were seeded in 6-well plates. When the cell density reached 70% confluence, only DMEM/F12 was used to replace the medium, and a mixture of transfection reagent containing Opti-MEM, ER β siRNA, FOXO3a siRNA or negative control siRNA (GenePharma, Shanghai, China) and Lipofectamine RNAiMAX (Invitrogen) were added dropwise to each well. After 6 h, the culture medium was replaced with normal culture medium, and after an additional 48 h, the cells were collected after culture. The siRNA sequences used were as follows: ER β sense: ATGATCAGCTGGGCCAAGAA (5' to 3'); ER β antisense: CCACATCAGCCCCATCATTA (5' to 3'); FOXO3a sense: CGGACAAACGGCTCACTCT (5' to 3'); and FOXO3a antisense: GGACCCGCATGAATCG ACTAT (5' to 3'). For overexpression of ER β and FOXO3a, the empty pENTER plasmid, empty pCMV plasmid, pCMV-ESR2 plasmid, or pENTER-FOXO3a plasmid (WZ Biosciences, Shangdong, China) was transfected into KGN cells with Lipofectamine 3000 transfection reagent (Invitrogen, Carlsbad, CA) according to the manufacturer's protocol. The procedure was similar to that described above. Cells were harvested for RNA or protein isolation after 48 h of incubation.

Quantitative real-time PCR (qPCR)

Total RNA was extracted using TRIzol reagent (Invitrogen) according to the manufacturer's instructions. The RNA was reverse transcribed into cDNA using an ABI High-Capacity cDNA Archive Kit (Applied Biosystems, Foster City, California), and real-time PCR was carried out on a 7500 Real-Time PCR System using 2 \times SYBR Green SuperMix (Invitrogen). The expression levels of the target genes relative to the internal parameters were calculated by the 2 $^{-\Delta\Delta Ct}$ method as follows: $\Delta Ct = \Delta Ct_{\text{target}} - \Delta Ct_{\text{reference}}$, $-\Delta\Delta Ct = -(\Delta Ct_{\text{treat}} - \Delta Ct_{\text{control}})$. The specific primers used for qPCR analysis are shown in Table 2. The primer specificity was verified by melting curve analysis. Actin was used as an internal reference gene.

Western blotting

The cells were lysed in RIPA buffer (Solarbio, Beijing, China) supplemented with 1 mM PMSF (Solarbio), and a BCA protein concentration assay kit (Solarbio) was used to measure the protein concentrations. Equal amounts of protein were separated via SDS–PAGE on a 10% gel and electroblotted onto polyvinylidene fluoride membranes (Millipore, Billerica, MA, USA). The membranes were blocked with 5% nonfat dry milk (Sangon Biotech, Shanghai, China) for 1 h and probed overnight at 4°C with primary antibodies. Anti-ER β (04842, 1:1000) was obtained from Merck Millipore. Anti-FOXO3a (D19A7, 12829, 1:1000), anti-Bcl2 (D40C5, 3495T, 1:1000) and anti-ATG7 (D12B11, 8558, 1:1000) were purchased from Cell Signaling Technology (MA, USA). Anti-LC3 (ab48394, 1:1000) and anti-cyclin D1 (ab16663, 1:1000) were purchased from Abcam (Cambridge, UK). Anti-BCL2 (A19693, 1:1000) and anti-BAX (A19684, 1:1000) were obtained from ABclonal (Wuhan, China). Anti-GAPDH (TA-08, 1:1000) and anti-actin (TA-09, 1:1000) were purchased from ZSGB-BIO (Beijing, China). After five washes in TBST, the membranes were incubated with

a secondary antibody, anti-mouse/rabbit IgG peroxidase-conjugated secondary antibody (Santa Cruz, CA, USA), conjugated with horseradish peroxidase for 1 h at 37°C. The protein bands were visualized with enhanced

chemiluminescence (ECL) solution (Syngene, Cambridge, United Kingdom). ImageJ software was used to analyse the intensities of the Western blot bands. The results were normalized with housekeeping genes.

Table 2. qPCR primers.

Gene	Direction	Primer
ERβ	Forward	5'-ATGATCAGCTGGGCCAAGAA-3'
	Reverse	5'-CCACATCAGCCCCATCATTAA-3'
FOXO3a	Forward	5'-CGGACAAACGGCTCACTCT -3'
	Reverse	5'-GGACCCGCATGAATCGACTAT-3'
Beclin1	Forward	5'-CCATGCAGGTGAGCTTCGT-3'
	Reverse	5'-GAATCTGCGAGAGACACCATC-3'
ATG7	Forward	5'-CTGCCAGCTCGCTTAACATTG-3'
	Reverse	5'-CTTGTTGAGGAGTACAGGGTTTT-3'
CyclinD1	Forward	5'-CTGTGCTGCGAAGTGGAAACCAT-3'
	Reverse	5'-TTCATGGCCAGCGGGAAGACCTC-3'
BCL2	Forward	5'-AAACTTGACAGAGGATCATGCTGTA-3'
	Reverse	5'-TGGCATGAGATGCAGGAAATT-3'
BAX	Forward	5'-CCCGAGAGGTCTTTTCCGAG-3'
	Reverse	5'-CCAGCCCATGATGGTTCTGAT-3'
Actin	Forward	5'-GTGGCCGAGGACTTTGATTG-3'
	Reverse	5'-CCTGTAACAACGCATCTCATATT-3'
ERβ mouse	Forward	5'-TTCTTTTCTCATGTCAGGCACA-3'
	Reverse	5'-CTCGAAGCGTGTGAGCATT-3'
FOXO3a mouse	Forward	5'-ACAAACGGCTCACTTTGTCCCAGA-3'
	Reverse	5'-TCTTGCCCGTGCCTTCATTCT-3'
Beclin1 mouse	Forward	5'-TGAAATCAATGCTGCCTGGG-3'
	Reverse	5'-CCAGAACAGTATAACGGCAACTCC-3'
ATG7 mouse	Forward	5'- TCTGGGAAGCCATAAAGTCAGG-3'
	Reverse	5'-GCGAAGGTCAGGAGAA-3'
Cyclin D1 mouse	Forward	5'-TCAAGTGTGACCCGGACTGC-3'
	Reverse	5'-CCTTGGGGTCGACGTTCTG-3'
BCL2 mouse	Forward	5'-CTTTGAGTTCGGTGGGGTC-3'
	Reverse	5'-GTTCCACAAAGGCATCCCA-3'
Actin mouse	Forward	5'-GTGACGTTGACATCCGTA-3'
	Reverse	5'-GTAACAGTCCGCCTA-3'

Transmission electron microscopy

GCs and KGN were fixed with glutaraldehyde (G5882; Sigma–Aldrich) and osmium tetroxide and postfixed with OsO₄ and sucrose. Then, graded concentrations of ethanol were used to dehydrate the cells. Subsequently, the samples were embedded in embed-812 dodecenylsuccinic anhydride, dimethylaminomethyl phenol and methyl nadic anhydride. Then, the 80-nm-thick sections were contrasted with lead citrate and uranyl acetate. A JEM-1400plus electron microscope was used to capture images. According to previously reported guidelines³¹, autophagosomes, also referred to as initial autophagic vacuoles, typically have a double membrane or a membrane at least partly visible as two parallel membrane bilayers under an electron microscope. Three patients were randomly selected from the DOR and

control groups, and autophagosomes in 15 different cells per patient were observed and counted by Lei Zhang, an experienced professor from Peking University. A total of 3 independent experiments were performed, and autophagosomes in 15 different KGN cells were observed and counted in each experiment.

Chromatin immunoprecipitation (ChIP)

KGN cells were cultured in 15-cm dishes. When the cell confluence reached 90%, a ChIP assay kit (Pierce Chromatin Prep Module; Thermo Scientific, MA, USA) was used according to the manufacturer's instructions. Briefly, cells were collected in PBS containing 1% protease inhibitors and crosslinked with 1% formaldehyde. The crosslinked cells were then cleaved by micrococcal nuclease and digested by enzymes to cut genomic DNA. A total of 5 μ L of the digested chromatin

(10% input) was stored at -20°C as the input control and was used for IP elution and DNA recovery. The remaining digested chromatin was immunoprecipitated with an anti-ER β antibody (04842, 1:200, Merck Millipore) with rotation at 4°C overnight with rotation, IP elution and DNA recovery. IgG was used as a negative control. The purified DNA was analysed by RT-qPCR. The sequences of the FOXO3a promoter primers used were as follows: (F) 5'-GCGTGCCTTGACGAG-3'; (R) 5'-CAAGCTAGTTCGACGCGTACAA-3'.

Luciferase assay

KGN cells were transfected with expression vectors encoding pcDNA3.1-ER β , the pGL3-FOXO3a promoter and the pGL3-FOXO3a site mutation promoter (Genomeditech, Shanghai, China) using LipofectamineTM 3000 transfection reagent. A 2 μg firefly luciferase reporter structure containing a FOXO3a promoter site mutation and 30 ng of the Renilla luciferase reporter plasmid pRL-TK were used as internal controls for each transfection. The cells were harvested 48 h post-transfection, and luciferase activity was measured with a luciferase assay system (Promega, WI, USA). The firefly luciferase activity in each well was normalized to the Renilla luciferase activity. The measurements were performed on cultured cells from 3 different subjects and repeated twice.

Cell treatment

After transfection with the indicated siRNA or plasmid for 24 h, KGN cells were treated with the autophagy inhibitor 3-methyladenine (3-MA) (5 mM, S2767, Selleck) or the autophagy inducer rapamycin (rapa) (100 nM, S1039, Selleck) for another 24 h, after which the following experiments were performed.

Flow cytometry analysis

Apoptosis was assessed using an Annexin V-FITC Apoptosis Detection Kit (BD Biosciences, USA). The cells were harvested after treatment, washed twice with cold PBS and binding buffer, and incubated in the dark for at least 15 min with Annexin V-FITC. Propidium iodide (PI) was added to the cells, which were incubated in the dark at room temperature for 10 min. Apoptosis was determined via flow cytometry. The degree of early apoptosis was determined by flow cytometry as the percentage of cells that were positive for Annexin V and negative for PI. Cells negative for Annexin V and PI were classified as normal. Cells that were positive for Annexin V and negative for PI were considered early apoptotic

cells. Annexin V- and PI-positive cells were considered late apoptotic cells.

Cell Counting Kit-8 (CCK-8) assay

Cell viability was analysed by the CCK-8 assay (Beyotime, Shanghai, China) according to the manufacturer's protocol. The cells were cultured at a density of 0.5×10^4 cells/well in 100 μL of medium in 96-well microplates (Corning, USA). After 24 h, 10 μL of CCK-8 reagent was added to each well, and the cells were then cultured for 2 h. All the experiments were performed in triplicate. The absorbance was analysed at 450 nm using a microplate reader (Bio-Rad, Hercules, CA, USA), and wells without cells were used as blanks. The proliferation of cells was assessed by measuring the absorbance.

Animal model

Female (7–8 weeks old) and male (8–9 weeks old) C57BL/6J mice and female (28–32 g) and male (10 weeks old) ICR mice were purchased from Beijing Vital River Laboratory Animal Technology Co., Ltd., and housed under specific pathogen-free (SPF) conditions at a controlled temperature ($22 \pm 1^{\circ}\text{C}$) and humidity ($60 \pm 10\%$) with ad libitum access to water and regular rodent chow on a 12 h light/12 h dark cycle. All animal protocols were approved by the Peking University First Hospital Animal Care and Use Committee (protocol number: J202141).

For construction of a cyclophosphamide (Cy)-induced DOR (Cy-DOR) model, 7- to 8-week-old C57BL/6 female mice were weighed and then given a single intraperitoneal injection of Cy (75 mg/kg, 200–300 μL) or an equal volume of saline as a control. Seven days later, we randomly divided the mice according to the conditions where the body weights of the mice in each group were matched. Then, the mice were administered PHTPP by intraperitoneal injection every other day for 14 days. The three groups were the DOR + PBS (vehicle), DOR + PHTPP (2 mg/kg, PHTPP2), and DOR + PHTPP (4 mg/kg, PHTPP4) groups. Serum and ovarian samples were collected after the mice were sacrificed. The weights of the mice and wet weights of the ovaries were measured (ovarian index = ovarian mass/mouse body weight \times 100%).

Evaluation of estrous cyclicity

Vaginal smears were collected from all of the mice daily at 9:00 am for 18 days and analysed via haematoxylin and eosin (H&E) staining. The stage of cyclicity was determined by the predominant cell type using

microscopic analysis. The four phases of the oestrus cycle are predominantly characterized by different cell types: nucleated epithelial cells are the predominant cells in the proestrus phase; cornified epithelial cells are the predominant cells in the oestrus phase; equal numbers of leukocytes, cornified epithelial cells and nucleated epithelial cells are present in the metestrus phase; and leukocytes are the predominant cells in the diestrus phase. Analysis of oestradiol (E2), FSH, luteinizing hormone (LH), and AMH levels by enzyme-linked immunosorbent assays (ELISAs)

After incubating for 2 h at room temperature, the mouse blood was centrifuged for 20 min at $2000 \times g$, after which the supernatant was collected. AMH, E2, FSH and LH levels were measured using an ELISA kit (Cusabio, Wuhan, China) according to the manufacturer's protocol. The results were analysed using a microplate reader (Bio-Rad, Hercules, CA, USA).

Histopathology and follicle counting

Ovaries were collected and fixed in 4% paraformaldehyde for 24 h. Then, the tissues were embedded in paraffin and sliced into 5 μ m thick pieces for H&E staining. Follicles were counted in every fifth serial section from ten mice in each group. The mean number per section was calculated. The follicles were counted at different stages while the sections were viewed under a Nikon digital microscope (Nikon, Melville, NY, USA). The follicles were classified as follows³²: primordial follicles consisted of one layer of flattened GCs surrounding the oocyte; primary follicles consisted of one to two complete layers of cuboidal GCs; secondary follicles consisted of more than one layer of cuboidal GCs with no visible antrum around an oocyte; and antral follicles consisted of an oocyte and multiple layers of cuboidal GCs and contained one or more antral spaces, possibly with cumulus oophores and a thecal layer.

Terminal deoxynucleotidyl transferase-mediated dUTP nick end labelling (TUNEL) staining

For analysis of apoptosis in ovarian tissue, deparaffinized tissue sections were permeabilized with 10 μ g/mL proteinase K in 10 mM Tris HCl and subjected to TUNEL staining according to the manufacturer's instructions (Proteintech, Wuhan, China). The samples were counterstained with 4',6-diamidino-2-phenylindole (DAPI, Molecular Probes). Sections were observed, and images were captured with an epifluorescence microscope (Axio Imager 2, Carl Zeiss) by the imaging program ZEN.

Superovulation induction and oocyte collection

For collection of MII oocytes, superovulation was induced in mice from the NC, Cy, and Cy+PHTPP groups by intraperitoneal injection of 10 IU of pregnant mare serum gonadotrophin (PMSG), followed by 10 IU of human chorionic gonadotropin (hCG) 48 h later. Cumulus-oocyte complexes (COCs) were collected from oviductal ampullae 15–17 h after hCG injection. MII eggs and cumulus cell complexes were collected from oviducts. After hyaluronidase (500 IU/mL) treatment, the cumulus mass was dissociated, and MII eggs were collected in M2 medium.

IVF and embryo culture

Epididymal spermatozoa were retrieved from the cauda epididymis of 12–15-week-old C57BL/6J male mice. The sperm suspensions were incubated in 10% serum protein substitute (SPS)/human tubal fluid (HTF) at 37°C in 5% CO₂ and 95% humidity for 90 min. Ovulated oocytes with intact cumulus masses were recovered from the oviducts and maintained in HTF. Then, capacitated sperm at a concentration of $1\text{--}2 \times 10^6/\text{mL}$ were added to COC droplets and cultured at 37°C in 5% CO₂ at 95% humidity. Twenty-four to twenty-eight hours later, the oocytes were removed and examined for fertilization. Fertilization was assessed by two pronuclei (2PN). Fertilized embryos were cultured to the blastocyst stage in M16 medium for 86–88 h, and development was evaluated every 24 h.

Surgical transfer of embryos into recipient mothers

Female ICR mice mated with vasectomized male ICR mice were used as recipient mothers. The day after a vaginal plug was observed was considered Day 1 of pseudopregnancy. Mice were anaesthetized using inhaled isoflurane (Steve Laboratories, UK). The uterine horn was exposed via a dorsal incision using tweezers. With a glass micropipette, 12 embryos per horn were transferred into the oviduct in a small volume of culture medium (M2). The expected perinatal period after 2-cell embryo transfer was 19 days. Female surrogate ICR mice gave birth near the end of the expected perinatal period, and the litter size of each mouse was recorded for comparison between groups.

Fertility assessment

C57BL/6J female mice were housed with demonstrably fertile C57BL/6 males (3 months old) at a 1:1 ratio, and the delivered offspring were assessed. The number of pups per litter and pup health were recorded and statistically analysed.

Reactive oxygen species (ROS) level analysis

Intracellular ROS levels were analysed using a Reactive Oxygen Species Assay Kit (Thermo, USA) according to the manufacturer's instructions. Briefly, a 5 μ M MitoSOX working solution was prepared. Degranulated MII oocytes from different groups were placed in MitoSOX working solution and incubated in a 5% CO₂ incubator at 37°C for 20-30 minutes in the dark. After being washed three times in M2 medium, the oocytes were observed under a Leica microscope. The fluorescence intensity (excitation at 488 nm) was measured. All images were taken using fixed microscope parameters, and the fluorescence intensity of each oocyte was analysed via ImageJ software.

Meiotic spindle staining

Degranulated MII oocytes were fixed in 4% paraformaldehyde at room temperature for 30 min,

permeabilized in 0.5% Triton X-100 for 20 min, blocked with 1% BSA dissolved in PBS and then incubated with an anti- α -tubulin antibody in a dark humidified chamber overnight at 4°C. The next day, the oocytes were washed with new BSA 3 times and incubated with an Alexa Fluor 488-conjugated secondary antibody (1:200, CST) for 1 h at room temperature (RT). Chromatin staining was performed by incubating the sections with 5 μ g/mL Hoechst 33342 (Sigma-Aldrich) for 5 min at room temperature. To confirm the specificity of the staining, isotype controls, the normal mouse IgG (SC-2025, Santa Cruz) and normal rabbit IgG (AB-105-C, R&D), instead of antibodies to specific proteins, were included in each experiment. There was no clear staining from these isotype controls was detected, suggesting that the signals are specific. Spindle and chromosome morphology were observed under an inverted laser confocal microscope with a water or oil lens.

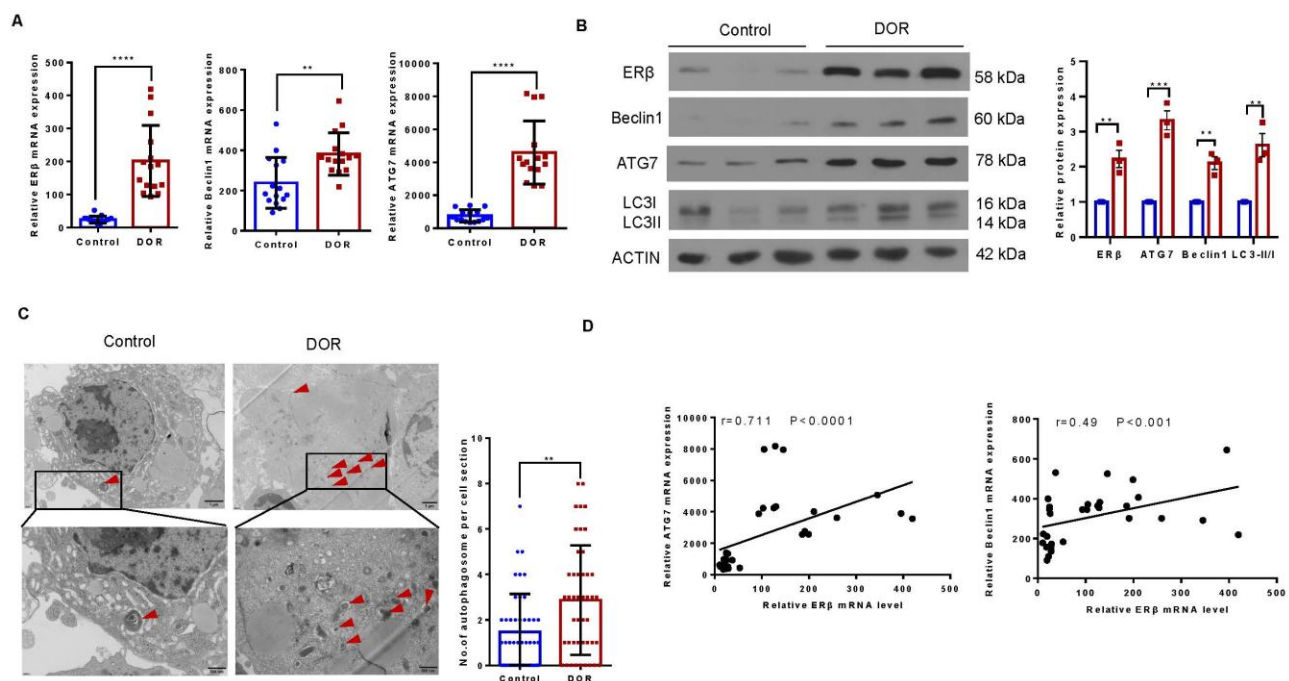


Figure 1. GCs from patients with DOR exhibit aberrant autophagy and increased ER β expression. (A) ER β , Beclin1 and ATG7 mRNA levels in GCs from the controls and patients with DOR were measured by qPCR ($n = 15$). (B) The expression of the ER β , ATG7, Beclin1 and LC3 proteins in GCs from the controls and patients with DOR ($n = 5$) was assessed by Western blotting, and representative results are shown. ACTIN was used as the loading control. (C) Transmission electron micrographs showing characteristic autophagosome formation (red arrows) in GCs from the controls and patients with DOR. The number of autophagosomes was counted in 15 randomly selected cells per patient ($n=3$). (D) The correlation of ATG7 and Beclin1 expression with ER β expression in GCs was analysed, and the linear regression coefficient and P value are shown ($n=30$). The data are presented as the mean \pm SEM. Statistical analyses for mRNA expression and autophagosome counts were carried out by two-tailed Student's t test. The P value for protein expression between two groups was from Mann-Whitney U test. The linear regression coefficient and P value were carried out by Spearman correlation analysis (** $P < 0.01$; **** $P < 0.0001$).

Statistical analysis

All the data are presented as the mean \pm SEM. All the statistical analyses were conducted using SPSS 26.0 software. Kolmogorov-Smirnov test and Q-Q plot were used to test the normality of the data using. If N is too small to determine normality, we used the non-parametric alternative (Mann-Whitney U test for 2 samples or Kruskal-

Wallis H test for more samples). Comparisons between two groups were performed using a two-tailed Student's t test. Comparisons among more than two groups were performed using one-way analysis of variance (ANOVA). Spearman correlation coefficients were calculated. P values < 0.05 were considered to indicate statistical significance.

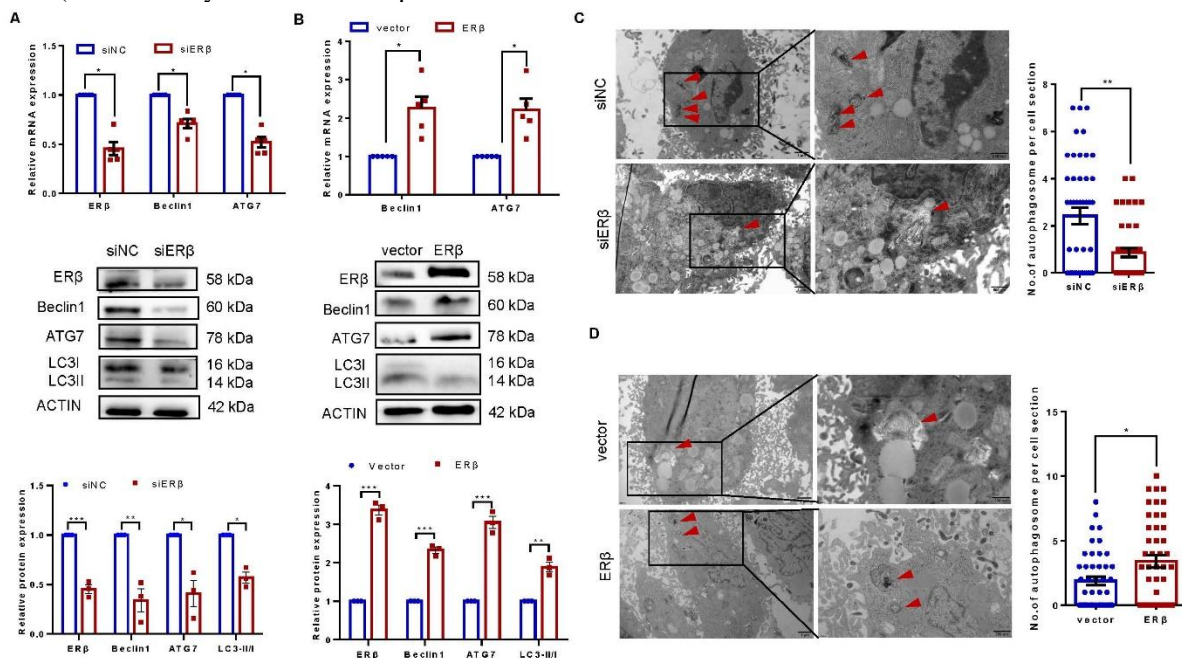


Figure 2. ER β induces autophagy in KGN cells. (A) KGN cells were transfected with ER β siRNA or control siRNA, and the levels of the indicated autophagy-related markers were measured via qPCR (n=5) or Western blotting (n=3). (B) KGN cells were transfected with an ER β overexpression plasmid or vector, and the levels of the indicated autophagy-related markers were measured via qPCR (n=5) or Western blotting (n=3). The efficiency of the knockdown or overexpression was verified by Western blotting (n=3) or qPCR (n=5). (C) KGN cells were transfected with ER β siRNA or control siRNA, and morphological examination was performed via transmission electron microscopy. The number of autophagosomes was counted in 15 randomly selected cells from each group (n=3). (D) KGN cells were transfected with the ER β overexpression plasmid or vector, and morphological examination was performed via transmission electron microscopy. The number of autophagosomes was counted in 15 randomly selected cells in each group (n=3). The data are presented as the mean \pm SEM. Statistical analyses were carried out by Mann-Whitney U test or two-tailed Student's t test (*P < 0.05; **P < 0.01; ***P < 0.001).

RESULTS

GCs from patients with DOR exhibit increased expression of ER β and autophagy

We examined the levels of ER β and autophagy-associated proteins in DORs and control GCs to determine their relationship and found that ER β expression was upregulated in GCs from patients with DOR. Moreover, upregulation of Beclin 1 (autophagy-related protein) and ATG7 (autophagy-related 7) and accumulation of the cleaved and lipidated form of MAP1LC3B-II/LC3B-II (microtubule-associated protein 1 light chain 3b) were also observed, indicating aberrant autophagic flux (Fig.

1A and B). Analysis via transmission electron microscopy analysis revealed that GCs from patients with DOR contained significantly more autophagosomes than did those from control patients (Fig. 1C). Moreover, a positive correlation was observed between ER β expression and Beclin1 and ATG7 expression in GCs (Fig. 1D). These data indicate that elevated ER β expression is positively correlated with the development of DOR associated with activated autophagy.

ER β induces autophagy in KGN cells

KGN cells were subjected to ER β gain-of-function and loss-of-function assays to examine the effects of ER β on

autophagy-related gene expression and autophagosome formation in GCs. We observed a decrease in the expression of autophagy-related genes, including ATG7, Beclin1, and LC3, at both the mRNA and protein levels upon ER β knockdown, while ER β overexpression induced their expression (Fig. 2A and B). Transmission

electron microscopy revealed that ER β overexpression increased the number of autophagosomes in KGN cells, while fewer autophagosomes were found in ER β knockdown cells (Fig. 2C and D). Taken together, these findings suggest that ER β enhances autophagy in KGN cells.

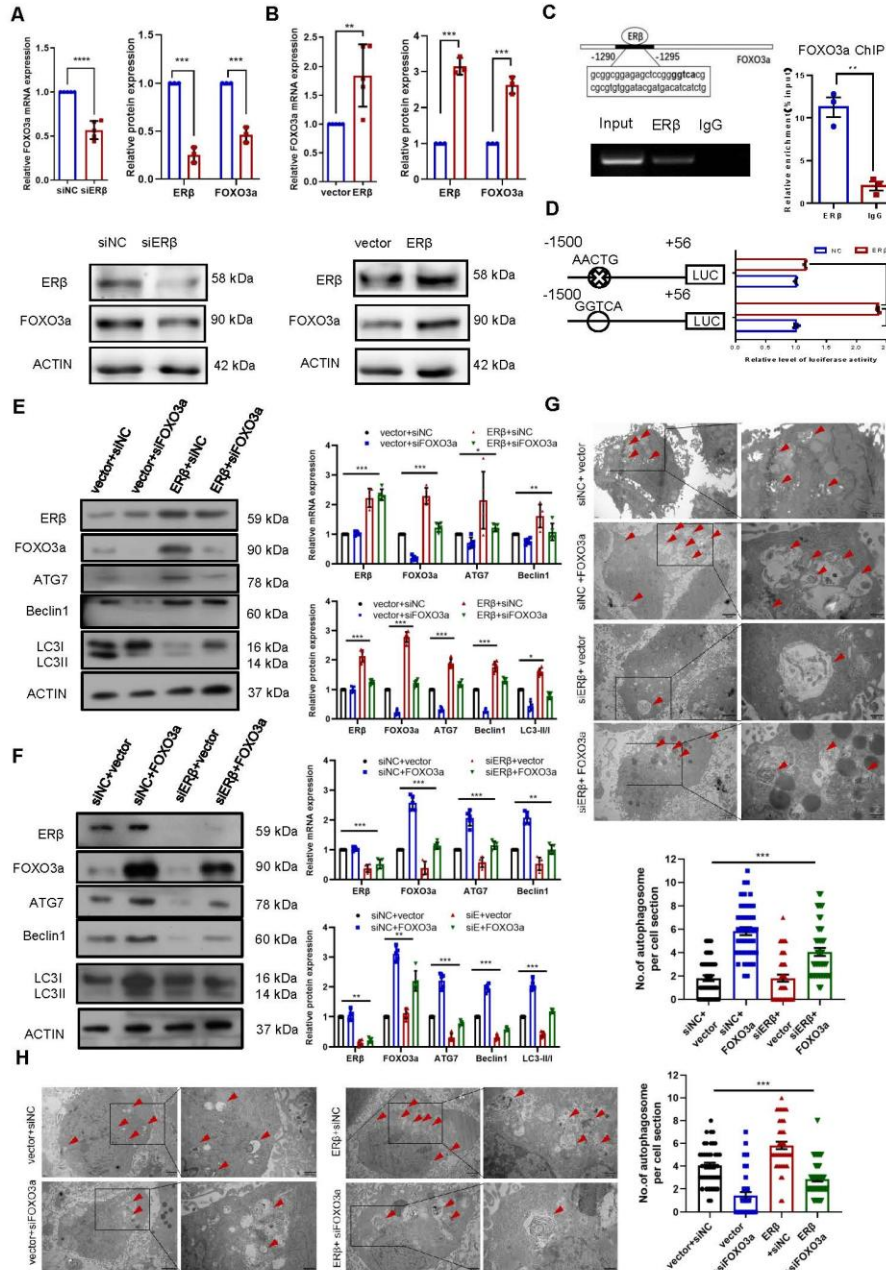


Figure 3. ER β -induced autophagy is mediated by FOXO3a.

(A) KGN cells were transfected with ER β siRNA or control siRNA, and FOXO3a expression was measured via qPCR (n=5) or Western blotting (n=3). (B) KGN cells were transfected with an ER β overexpression plasmid or vector, and FOXO3a expression was measured via qPCR (n=5) or Western blotting (n=3). (C) KGN cells were harvested and subjected to ChIP using an anti-ER β or control IgG antibody, followed by SYBR Green-based qPCR (n = 3). (D) Reporter plasmids containing the FOXO3a promoter with either a wild-type sequence or a mutated sequence were transiently transfected into KGN cells, after which luciferase activity was measured. The sequences of the indicated mutants were identical to the wild-type sequence except as shown (n = 3). (E, F) KGN cells were transfected with the indicated expression constructs and/or siRNAs, and autophagy-related gene expression was measured by qPCR and Western blotting. The efficiency of the knockdown and overexpression was verified by Western blotting or qPCR. (G, H) KGN cells were transfected with the indicated expression constructs and/or siRNAs, and morphological examination was performed via transmission electron microscopy. The number of autophagosomes was counted in 15 randomly selected cells from each group (n=3). The data are presented as the mean \pm SEM. Statistical analyses were carried out by Mann-Whitney U test or two-tailed Student's t test (*P < 0.05; **P < 0.01; ***P < 0.001; ****P < 0.0001).

ER β -induced autophagy is mediated by FOXO3a

Studies have shown that both ER β and FOXO3a are involved in POF development³³, and FOXO3a has been verified to be associated with cell autophagy³⁴; thus, we investigated whether FOXO3a participates in the regulation of autophagy induced by ER β in GCs. Previous

studies have suggested that ER β can upregulate FOXO3a expression in prostate cancer³⁰. Consistent with these findings, the expression of FOXO3a was decreased (Fig. 3A) by ER β knockdown but increased (Fig. 3B) by ER β overexpression. As a transcription factor, ER β directly regulates the transcription of target genes by binding to estrogen response elements (EREs) in promoter regions.

To achieve this goal, we utilized the UCSC (<http://genome.ucsc.edu/>) and JASPAR (<http://jaspardev.genereg.net/>) databases to determine the FOXO3a promoter sequence. In this study, we could not find any typical EREs with the sequence 5'-GGTCAnnnTGACC-3' 35 in the FOXO3a promoter. However, we did discover a potential site for ER β binding (half-ERE) at -1295/-1290 (Fig. 3C). We conducted a ChIP assay to investigate whether ER β can bind to the FOXO3a promoter region in KGN cells. ER β bound to the FOXO3a promoter (Fig. 3C). To validate that ER β regulates FOXO3a promoter activity, we carried out dual luciferase reporter assays. The results revealed that the promoter activity of the variant with a mutation within the -1295/-1290 region (GGTCA to AACTG) was significantly reduced by 50% compared to that of the wild-type construct (Fig. 3D). Thus, these results indicate that the transcriptional

regulatory element ERE, located at -1295/-1290 in the FOXO3a promoter, plays a crucial role in controlling FOXO3a expression in KGN cells.

To further determine whether ER β affects autophagy via FOXO3a, we first found that FOXO3a knockdown (Fig. 3E and H) reduced autophagy-related gene expression and autophagosome formation, while overexpression (Fig. 3F and G) had the opposite effect. Then we performed rescue experiments and found that ER β knockdown reduced ATG7, Beclin1, and LC3 expression, and autophagosomes were effectively eliminated by simultaneous overexpression of FOXO3a (Fig. 3F, G). In contrast, the upregulation of the above genes and the increase in autophagosomes caused by ER β overexpression could be rescued by depletion of FOXO3a (Fig. 3E, H). These observations support the notion that ER β affects GC autophagy through FOXO3a.

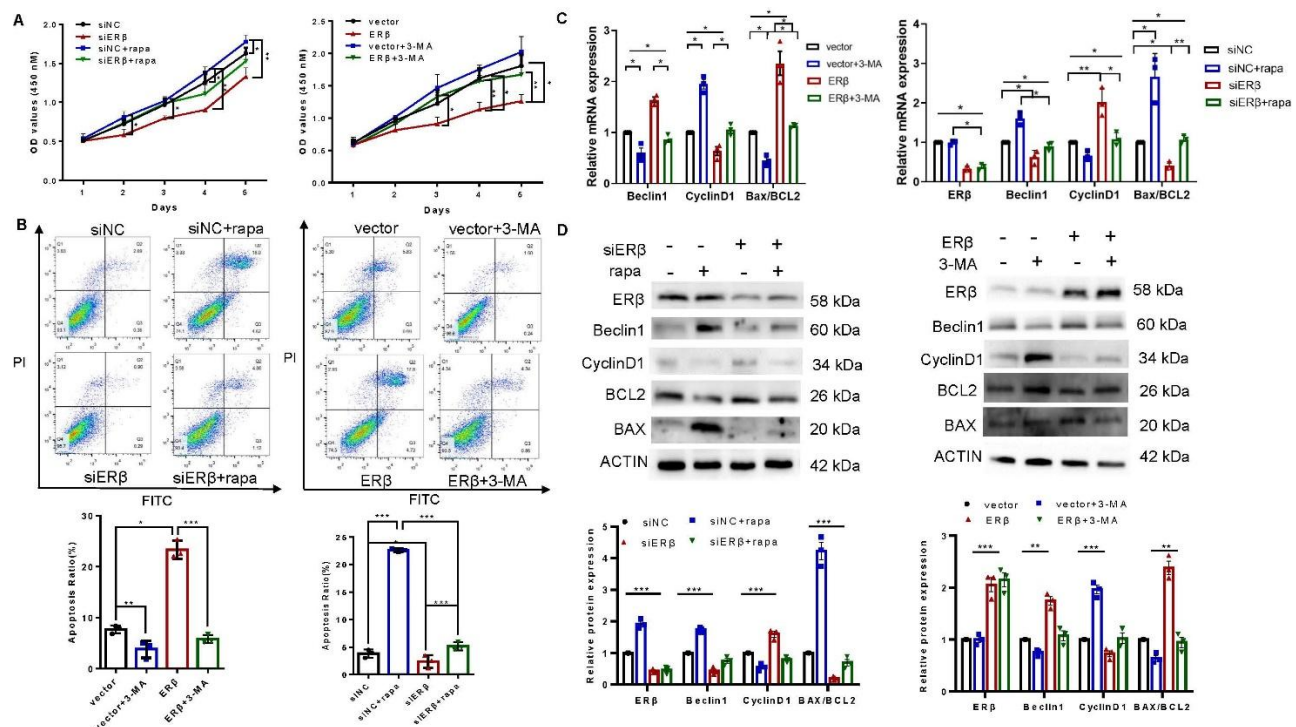


Figure 4. ER β promoted cell apoptosis and inhibited cell proliferation by inducing autophagy. After transfection with the indicated siRNA or plasmid for 24 h, KGN cells were treated with 3-MA or rapa for another 24 h. (A) CCK-8 assays were performed to measure KGN cell proliferation ($n = 3$). (B) Flow cytometry analysis was performed to determine the effect of ER β and autophagy on KGN cell apoptosis. The rate of apoptosis was determined ($n = 3$). (C, D) The mRNA and protein expression levels of the indicated proliferation- and apoptosis-related markers were assessed using qPCR and Western blotting ($n = 3$). The data are presented as the mean \pm SEM. Statistical analyses were carried out Mann-Whitney U test. (* $P < 0.05$; ** $P < 0.01$; *** $P < 0.001$).

ER β promotes cell apoptosis and inhibits cell proliferation by inducing autophagy

We next investigated how ER β affects GC function using loss- and gain-of-function experiments. Silencing ER β significantly promoted the proliferation of KGN cells, while ER β overexpression had the opposite effect, as

shown by the CCK-8 assay (Fig. 4A). Moreover, flow cytometry showed that ER β could facilitate apoptosis, and ER β deficiency led to a significant decrease in the percentage of apoptotic cells among GCs (Fig. 4B). Furthermore, we assessed the levels of apoptosis and proliferation markers. Silencing ER β led to an increase in the ratio of BCL2/BAX and in the expression of cyclin D1

(Fig. 4C and D). Upon forced expression of ER β in KGN cells, the ratio of BCL2/BAX and the expression of cyclin D1 decreased (Fig. 4C and D). To explore the relationship between ER β -mediated autophagy and apoptosis/proliferation, we used rapa and 3-MA. Rapa treatment significantly attenuated the increase in proliferation (Fig. 4A) and decrease in apoptosis (Fig. 4B) and markedly reversed the changes in the BCL2/BAX ratio and the

expression of cyclin D1 (Fig. 4C and D) induced by ER β knockdown. In contrast, 3-MA abolished the abovementioned alterations induced by ectopic expression of ER β (Fig. 4A, B, C, and D). Overall, these results suggest that ER β triggers cell apoptosis and inhibits cell proliferation in an autophagy-dependent manner.

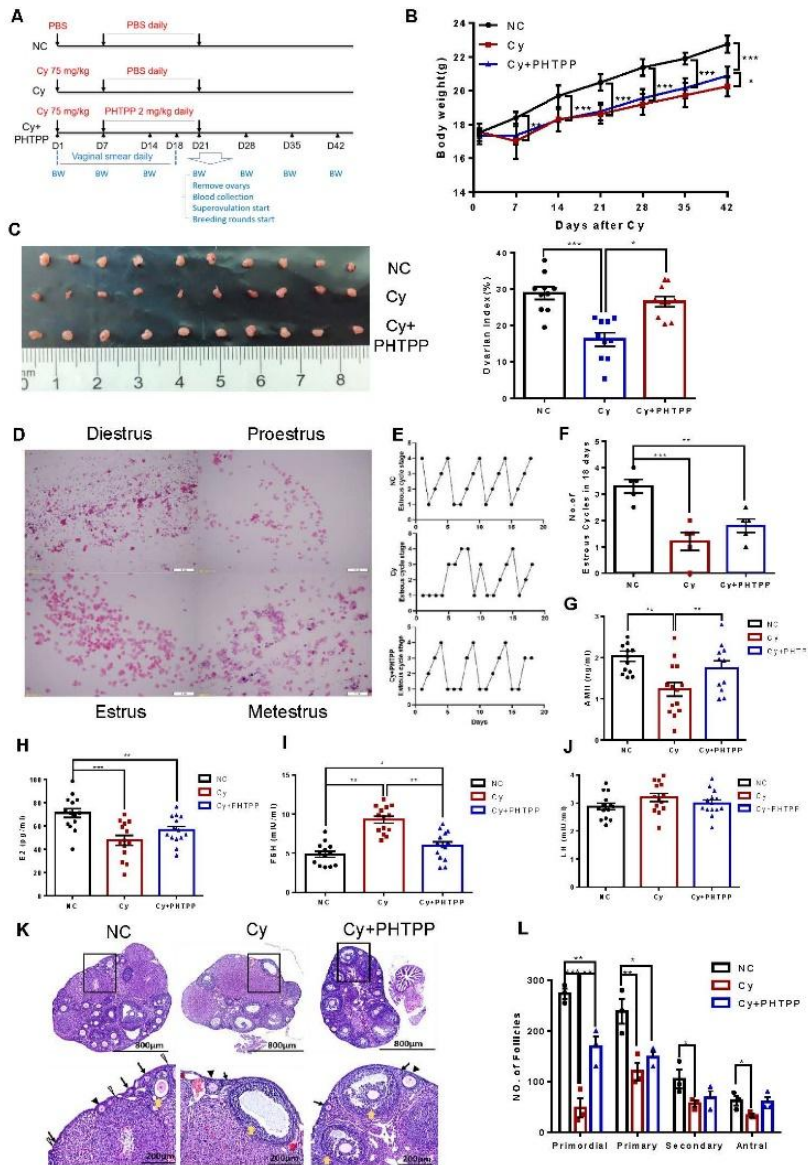


Figure 5. PHTPP rescued ovarian damage induced by Cy. (A) Design of the experiment in which Cy-induced DOR model mice were treated with PHTPP. (B) Changes in body weight in each group on days 1, 7, 14, 21, 28, 35 and 42 (n=12). (C) Comparison of ovarian morphology and the ovarian indices (ovarian weight [mg]/body weight [g]×100%) (n=10). (D) Morphology of typical cells in vaginal smears from mice during different phases of the oestrous cycle following H&E staining; scale bar: 1 mm. (E) The oestrous cycle of the mice was observed continuously for 18 days. A representative oestrous cycle from one mouse from each group is shown. The numbers on the x-axis indicate the following: 1, diestrus; 2, proestrus; 3, oestrus; and 4, metestrus. (F) During the 18-day observation period, the number of complete oestrous cycles of mice in each group was quantified (n=5). (G–J) The levels of AMH, E2, FSH and LH in the serum collected from the three groups were measured via ELISAs (n = 13–14 mice per group). (K) Representative images of H&E-stained ovaries from the different groups. Scale bars: 500 μ m, 200 μ m; white triangle: primary follicle; black arrow: primary follicle; black triangle: secondary follicle; yellow arrow: antral follicle. (L) The number of follicles in the different stages in ovary sections from the indicated groups was counted (n = 3 for each group). The data are presented as the mean \pm SEM. Statistical analyses were carried out Tamhane T2 test or Kruskal-Wallis H test. (*P < 0.05; **P < 0.01; ***P < 0.001).

PHTPP rescued ovarian damage induced by Cy

To verify whether the ER β antagonist PHTPP has a therapeutic effect on DOR in vivo, we established a DOR mouse model in female mice (6–8 weeks old, C57BL/6J) by administering a single intraperitoneal dose of Cy (75 mg/kg, 200–300 μ L) for 7 days. As shown in Supplementary Figure 1A, the Cy group had a lower

ovarian index and follicle count than did the NC group among female mice with DOR according to histological and morphometric analyses Supplementary (Fig. 1B). After confirming the successful establishment of the DOR model, we determined the protein and mRNA expression of ER β in ovarian tissues by Western blotting and qPCR analysis (Supplementary Fig. 1C and D). The protein expression of ER β was upregulated in ovarian tissues

from mice with DOR. Consistent with the Western blot results, the qPCR results confirmed that Cy exposure increased the mRNA expression of ER β . Therefore, ER β levels were elevated in the ovarian tissues of mice with

DOR, which was consistent with what was observed in the GCs of patients with DOR.

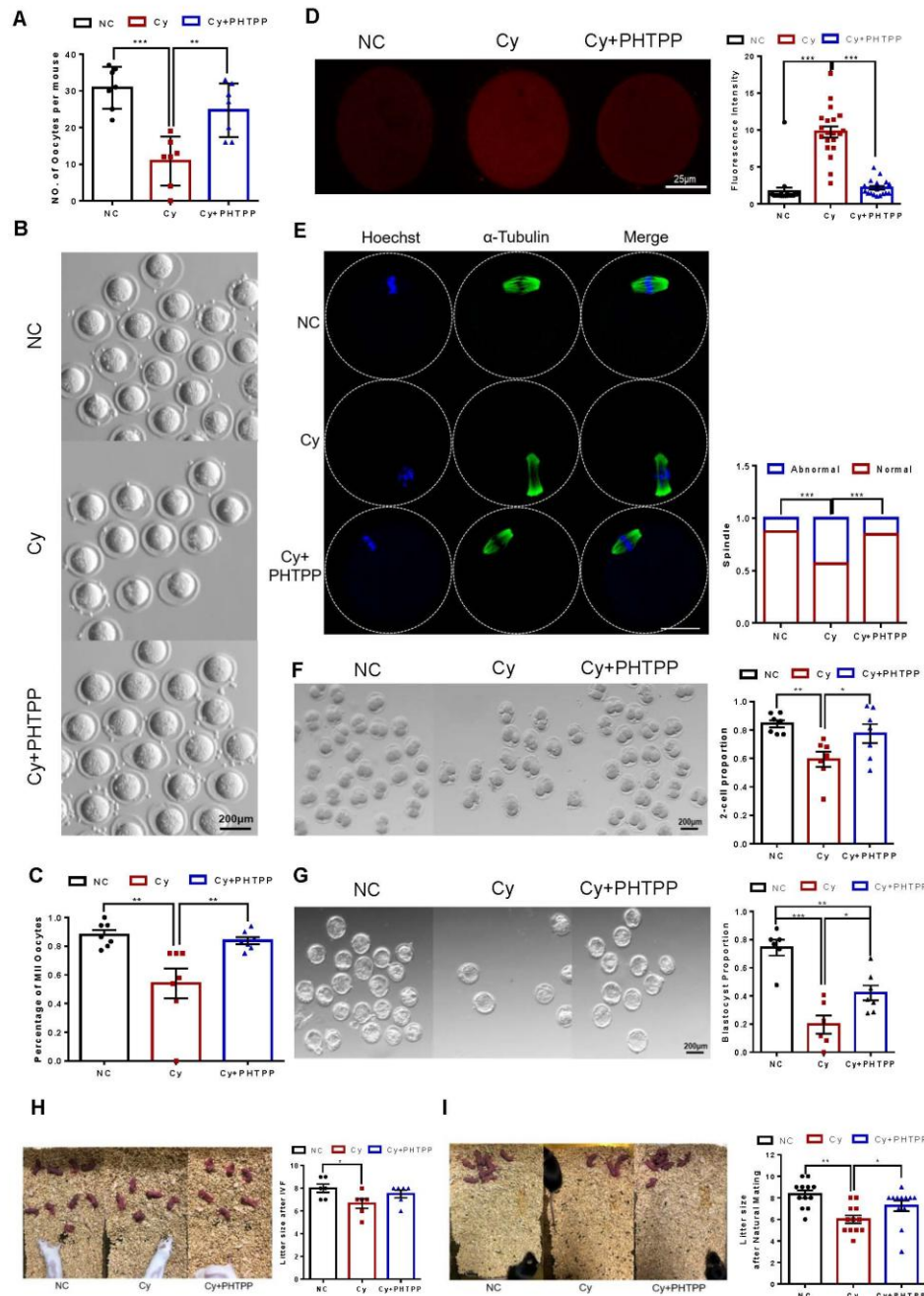


Figure 6. PHTPP reversed infertility in the Cy-induced DOR model. (A) Quantification of ovulated oocytes per mouse in each treatment group (n = 7 mice per group). (B) Morphology of MII oocytes from mice in each group; scale bars: 50 μ m. (C) Quantitative analysis of MII oocytes in each treatment group (n=7). (D) Measurement of intracellular ROS levels in MII oocytes using MitoSOX staining (red fluorescence); the relative fluorescence intensity was measured (n=20). Scale bars: 25 μ m. (E) Confocal microscopy results showing the assembly of spindles collected from cultured MII oocytes in each group. Scale bars: 25 μ m. The proportion of abnormal MII oocytes with a deformed spindle and misaligned chromosomes was quantified (n=59-73). (F) Representative images of 2-cell embryo morphology and statistical analysis of the 2-cell embryo formation rate in the different groups after IVF (n=7). Scale bars: 50 μ m. (G) Schematic diagram of blastocyst morphology and comparison of blastocyst formation rates among groups (n=6-7). Scale bars: 50 μ m. (H) Quantification of the mean litter size after IVF-ET (n=6). (I) Quantification of the mean litter size after natural mating (n=12). Statistical analyses were carried out by Tamhane T2 test. (*P < 0.05; **P < 0.01; ***P < 0.001).

After 7 days of DOR induction, the mice were subjected to daily intraperitoneal (i.p.) treatment with PHTPP or vehicle for 14 days (2 mg/kg or 4 mg/kg). Our preliminary experiment revealed that both doses could restore the ovarian reserve (Supplementary Fig. 1E, F and G). Then, based on the results and the principle of

minimizing the dosage of drugs, we evaluated the blood physiology and biochemical indices of the mice after intraperitoneal injection at 2mg/kg PHTPP, and the results showed that, compared with those in the NC group, PHTPP itself had little toxicity to the animals and that there were no obvious abnormalities (Supplementary Fig.

1H and I). Thus, we selected 2 mg/kg PHTPP for treatment (the group that received this treatment was referred to as the Cy+PHTPP group).

Animal experiments were performed according to the experimental timeline presented in Figure 5A. After PHTPP treatment, mice in the Cy+PHTPP group exhibited gradual weight gain and significant increases in both ovarian weight and the ovarian indices, as shown in Figure 5B and C. We subsequently monitored the oestrous cycle, and the results showed that PHTPP partially restored the estrous cycle in mice with DOR (Fig. 5D and F). Treatment with PHTPP reversed the abnormalities in blood AMH and FSH levels but had no effect on E2 or LH levels (Fig. 5G, H, I and J). Moreover, ovarian morphology was compared among the NC, Cy, and Cy+PHTPP groups, and H&E staining (midline sections) of ovaries showed that PHTPP treatment significantly alleviated Cy-induced damage to ovarian follicles, contributing to their normal development (Fig. 5K and L). Quantitative analysis revealed that treatment with PHTPP reduced the Cy-induced decrease in primordial and primary follicle counts (Fig. 5L). Taken together, these results indicate that PHTPP can rescue ovarian damage induced by Cy.

PHTPP reverses infertility in the Cy-induced DOR model

In mammals, the development of both oocytes and follicles regulates the reproductive capacity of females³⁶. The number and quality of oocytes are crucial for fertility. Administering PHTPP increased the number of ovulated oocytes, as shown in Fig. 6A. For evaluation of the developmental potential of the oocytes, germinal vesicle (GV) oocytes from the NC, Cy, and Cy+PHTPP groups were isolated and cultured in vitro. The MII rate of Cy oocytes was significantly decreased, while there were no differences in the MII rate between Cy+PHTPP and NC group oocytes (Fig. 6B and C). Furthermore, we examined the level of ROS in the NC, Cy and Cy+PHTPP groups of oocytes. Cy mice exhibited significantly increased ROS production, and a dramatic decrease in ROS levels was observed in oocytes from the Cy+ PHTPP group (Fig. 6D). In addition, abnormal spindle assembly, loss of normal morphology, loss of polarity and disordered chromosome arrangement were observed in oocytes from the Cy-treated mice (Figure 6E). However, the percentage of MII oocytes exhibiting abnormal spindles was significantly lower in the mice treated with Cy+PHTPP (Fig. 6E). These results indicate that the increase in ER β levels not only impairs follicular development but also alters oocyte development.

To explore the developmental potential of oocytes in the different groups, we conducted IVF using a previously

described method³⁷. The results showed that the rate of 2-cell embryo formation was notably lower in the Cy group than in the NC group. However, the level was significantly greater than that in the Cy+PHTPP group (Fig. 6F). Then, 2-cell embryos were cultured in vitro, after which the blastocyst formation rate was calculated. The results showed that the blastocyst formation rate of the mice in the Cy group was also significantly lower than that of the mice in the NC group and was significantly greater after PHTPP treatment (Fig. 6G). IVF-ET and mating trials were subsequently performed to further determine the protective effect of PHTPP on fertility. We observed that the litter size (number of pups per litter) in the Cy group was notably lower than that in the NC group after IVF-ET (Fig. 6H), while the litter size in the PHTPP-treated group was greater than that in the Cy group; however, the difference was not significant (Fig. 6H). Furthermore, compared with those of the NC group, the litters of the Cy group exhibited a reduced size after natural mating. Importantly, this change in litter size was reversed by PHTPP treatment (Fig. 6I). These results suggest that the Cy-induced fertility defects can be effectively rescued by PHTPP treatment.

Effects of PHTPP on autophagy and apoptosis in the ovaries of DOR model mice

In the Cy group, many follicles exhibited significant GC apoptosis. However, these changes were not as severe in the ovaries of mice that received PHTPP treatment, as illustrated in Figure 7A. We quantified the labelled cells after TUNEL staining. The results indicate that, compared with the control treatment, Cy treatment increased the number of TUNEL-positive follicles, which is an indicator of an increased apoptotic index. PHTPP protected against this increase in the apoptotic index, as the apoptotic index of follicles from the Cy + PHTPP group was significantly lower than that of follicles from the Cy group and similar to that of follicles from the control group.

We analysed the expression of genes related to the FOXO3a/autophagy pathway, apoptosis, and proliferation in mouse ovaries following Cy treatment with or without PHTPP to examine follicle activation mechanisms. Cy treatment resulted in an increase in FOXO3a, ATG7 and Beclin1 expression, but PHTPP inhibited this increase (Fig. 7B). Furthermore, PHTPP treatment increased the expression of Bcl-2 (Fig. 7B), suggesting that PHTPP inhibited the decrease in follicle count caused by Cy-induced apoptosis. Similar effects on the protein levels of the above genes were also observed (Fig. 7C). These results further suggest that PHTPP can reduce autophagy and apoptosis and promote proliferation in the ovaries of mice with DOR. The present study suggested that the

therapeutic effects of PHTPP in humans are comparable to those in mice.

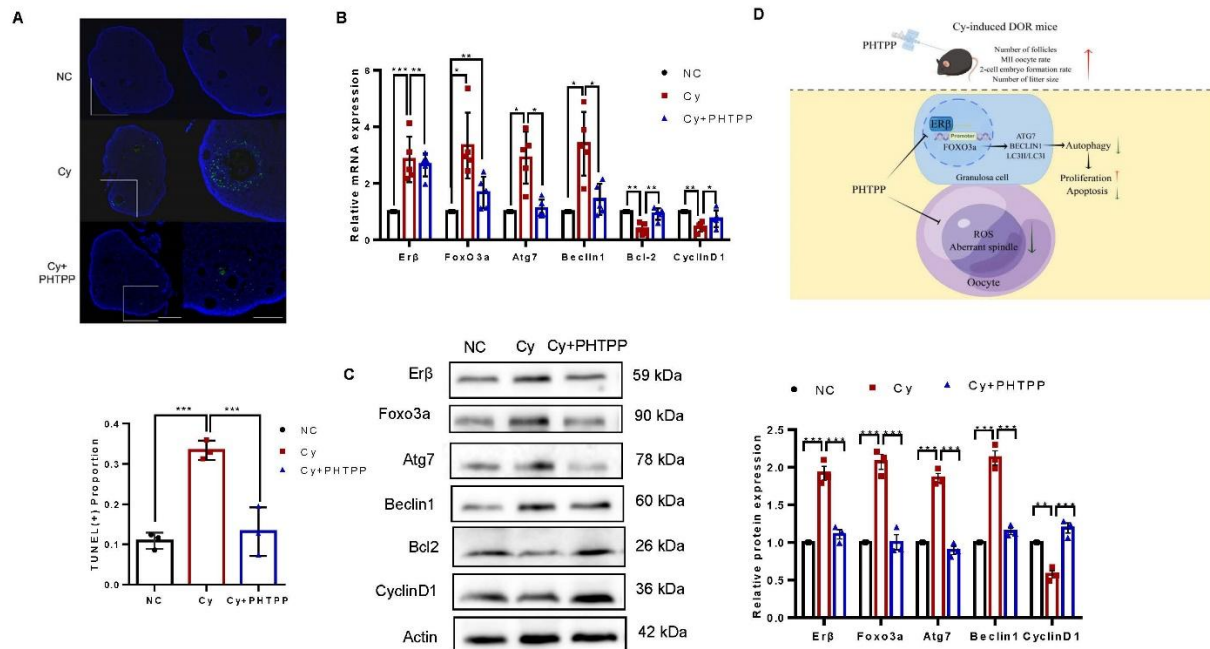


Figure 7. Effects of PHTPP on apoptosis and autophagy in the ovaries of DOR model mice. (A) TUNEL staining was performed to evaluate GC apoptosis in the ovaries of each treatment group, and TUNEL-positive cells in the ovarian sections were quantitatively analysed ($n = 3$ for each group). Scale bars: 500 μ m, 200 μ m. (B, C) Ovaries were obtained from mice in each treatment group. The mRNA and protein expression levels of Er β , Foxo3a, Atg7, Beclin1, Bcl-2 and Cyclin D1 were measured by qPCR ($n=5$) and Western blotting ($n=5$). (D) Schematic showing the role of ER β in the regulation of FOXO3a/autophagy signalling in GCs. Statistical analyses were carried out by Kruskal-Wallis H test. (* $P < 0.05$; ** $P < 0.01$; *** $P < 0.001$).

DISCUSSION

In recent years, the occurrence of DOR has been increasing, and DOR tends to affect younger patients¹. DOR is a popular research topic in the field of reproductive health, and different techniques, including mitochondrial transplantation, primordial follicle activation, in vitro follicle culture and stem cell transplantation, are being explored to improve the quality and quantity of oocytes in patients with DOR³⁸⁻⁴⁰; however, there are still no ideal treatment options available for women who suffer from DOR. In this study, we found for the first time that ER β /FOXO3a/autophagy plays an important role in the etiopathogenesis of DOR. Moreover, a selective ER β antagonist, PHTPP, was found to partially improve ovarian function and pregnancy outcomes in Cy-induced DOR model mice. Taken together, these results demonstrate that PHTPP has beneficial effects on a mouse model of DOR and provide an experimental basis for further exploration of its therapeutic potential in patients with DOR.

DOR refers to a decrease in the number and/or quality of oocytes. The number of oocytes is affected by the size of the primordial follicle pool, follicle growth and

development, maturation, ovulation and follicle atresia¹. Follicular atresia is a crucial selective process in the development of mammalian ovarian follicles and is the main cause of oocyte loss, which occurs in association with GC death¹⁶. Autophagy is a highly regulated intracellular process that helps maintain cellular homeostasis, protects against starvation, aids in differentiation, and supports normal growth⁴¹. Increasing evidence indicates that autophagy in GCs is involved in follicular atresia⁴². Choi et al. reported that autophagy is induced mainly in GCs during follicular atresia, leading to apoptotic cell death^{15, 43}. These findings imply that autophagy plays a direct role in follicular atresia and has a negative effect on the ovarian reserve. Over the years, multiple reports have indicated that autophagy plays a role in regulating oocyte survival and the formation of primordial follicles. However, conflicting results have been reported by different groups, and the findings seem to be dependent on various factors, such as the type of mouse strain used, the method of inducing or inhibiting autophagy, the concentration of the agent used, and the duration of exposure⁴⁴. Therefore, assessing the difference in autophagy levels between GCs from patients with DOR and those from patients with normal ovarian

reserve function is crucial for revealing the effect of autophagy on the ovarian reserve. We found that the expression of the autophagy-related factors ATG7 and Beclin1 and the LC3II/LC3I ratio were increased in the GCs of patients with DOR, suggesting that autophagy was overactivated. The above results were further confirmed by electron microscopy. However, the molecular pathways controlling the induction of autophagy in GCs are unclear.

In the ovary, GCs are responsible for estrogen synthesis⁴⁵. Research has demonstrated that ER β is the major oestrogen receptor isoform in the adult female ovary, particularly in GCs^{24, 25}; therefore, it is highly probable that ER β plays an important role in the regulation of ovarian function. At present, findings related to the effect of ER β on the ovarian reserve are inconsistent. On the one hand, ER β may play a crucial role in maintaining the primordial follicle pool. A study on the effect of gamma radiation on the ovarian reserve in rats revealed that upregulation of ER β expression in the ovary could inhibit the transition of primordial follicles to more growing follicles and promote GC proliferation⁴⁶. On the other hand, ER β inhibits GC and oocyte development. Nerve growth factor affects intracellular signalling cascades and cyclin integration by suppressing ER β expression, thereby inhibiting GC proliferation and affecting follicle quality⁴⁷. Another study revealed that activation of ER β during mid-pregnancy in mice results in delayed primordial follicle development after birth, impaired follicle development after prepuberty, and ultimately a reduced total litter size⁴⁸. Furthermore, studies involving *Esr2*^{-/-} rats have suggested that ER β plays a gatekeeping role in maintaining primordial follicle activation⁴⁹. In our current research, we also discovered that ER β may have a detrimental effect on ovarian reserve. We observed a significant increase in ER β expression in both patients with DOR and Cy-induced DOR model mice, but the specific regulatory mechanism involved is still unclear.

The autophagy-inducing function of ER β has been confirmed in various cell types, such as osteosarcoma cells and human seminoma cells^{26, 29}. In breast cancer cells, ER β can increase autophagic flux by reducing the expression of BCL-2 and promoting cancer cell death⁵⁰. However, the relationship between ER β and autophagy in human or mouse GCs or ovaries has not been reported. Here, we found that ER β can activate autophagy in GCs, promote cell apoptosis and inhibit cell proliferation through autophagy, suggesting that the decrease in the ovarian reserve caused by high ER β expression is achieved by the promotion of autophagic death in GCs.

Subsequently, we investigated the molecular mechanisms of ER β -regulated autophagy in GCs. In breast cancer cells and prostate cancer cell lines, ER β can

upregulate FOXO3a expression, but the mechanism is not yet clear^{30, 51}. FOXO3a is an important intraovarian signalling molecule that negatively regulates oocyte growth and follicular development. Research has shown that the FOXO3a protein contributes to follicular atresia in mammalian ovarian GCs and oocytes by promoting apoptosis^{22, 52}, suggesting that FOXO3a might be a candidate gene for the development of DOR. Consistent with our hypothesis, patients with DOR exhibited high FOXO3a expression, and FOXO3a expression was positively correlated with ER β expression. Given these findings, we further demonstrated that ER β can play a role in transcriptionally activating FOXO3a and that the ERE sequence located at -1290/-1295 in the FOXO3a promoter is crucial for regulating FOXO3a expression. Additionally, FOXO3a is a potent transcriptional activator that induces the expression of autophagy-related genes. FOXO3a can regulate autophagy in skeletal muscle cells by transcriptionally activating autophagosome formation-related genes, including LC3 and Beclin1⁵³. Moreover, ATG7, a gene involved in autophagy, is regulated by FOXO3a in non-small cell lung cancer cells⁵⁴. The above study suggested that FOXO3a regulates autophagy by controlling the expression of autophagy-related genes. However, whether FOXO3a affects ovarian and GC quality by changing the level of autophagy and subsequently affecting ovarian reserve function has not been studied. In this study, we discovered that ER β targets FOXO3a to stimulate autophagy in ovarian GCs.

Then, the ER β -specific antagonist PHTPP was administered, and its therapeutic effect on mice with DOR was evaluated *in vivo*. PHTPP has been proven to effectively treat breast cancer and endometriosis both in laboratory and animal studies^{55, 56}. We investigated the therapeutic effect of this herb on DOR for the first time. The DOR animal model is relatively mature and variable and includes mainly chemical drugs, radiation, genetic knockout, and the induction of ovarian immune inflammation⁵⁷⁻⁶⁰. Considering the reproducibility, time consumption, success rate and other factors, the Cy modelling method for chemical drugs is relatively mature, reliable, simple, and feasible, has a short construction period, can provide a window for subsequent administration of therapeutic drugs, and is widely used in basic research⁶¹⁻⁶³. Therefore, in the present study, intraperitoneal injection of Cy was chosen to establish a DOR model. Our results, as well as those of previous studies⁶⁴, indicate that treatment with 75 mg/kg Cy induces DOR-like damage to the ovary. The ovarian index is the ratio of the ovarian wet weight to the body weight and is one of the indices used to evaluate ovarian function⁶⁵. This study revealed that PHTPP can increase the ovarian index, suggesting that PHTPP can ameliorate

ovarian atrophy caused by Cy and restore ovarian function to a certain extent. Cy has been reported to affect the secretion of steroid hormones by increasing apoptosis and altering follicular development, leading to ovarian dysfunction⁶⁶, which manifests as low levels of E2 and high levels of FSH⁶⁷. The results we observed in this study were consistent with those of the above studies, as PHTPP reduced the serum FSH level and increased the serum E2 level in mice with DOR, indicating that PHTPP helps to improve and restore ovarian endocrine function. AMH is a reliable marker of ovarian reserve and can indicate follicle pool size⁶⁸. We discovered that the decrease in primordial and primary follicles in the Cy group correlated with lower levels of serum AMH. After the administration of PHTPP, the number of primordial follicular pools was restored, and the AMH level was increased, suggesting that PHTPP restored the ovarian reserve to some extent.

Both reduced oocyte quantity and quality can lead to DOR. Cytotoxicity of Cy can lead to apoptosis of follicles at all levels. Although oocyte apoptosis induced by DNA damage resulting from Cy generally occurs within 2 days, GC damage has a superimposed effect on follicle development, leading to premature atresia of follicles and prolonged duration of apoptosis. This phenomenon is also the reason why ovarian GC apoptotic signals can be detected 2-3 weeks after the administration of Cy^{64, 69, 70}. In the present study, more apoptotic follicles containing many TUNEL-positive GCs were observed in the 75 mg/kg Cy group than in the control group, and the level of Bcl-2, which suppresses apoptosis, was also reduced in the ovaries. After PHTPP treatment, apoptosis was decreased in mice with DOR, suggesting that in addition to ER β expression, ovarian apoptosis was also inhibited in mice with DOR, thus alleviating the adverse effects on follicular development. Furthermore, there are many factors that cause oocyte quality to decrease, including increased oxidative stress, faulty spindle assembly, mitochondrial dysfunction, gene mutations, meiotic abnormalities, and decreased chromosome cohesion⁷¹. All of these factors can adversely affect oocyte development individually or collectively. In the present study, the administration of the ER β inhibitor PHTPP reduced the ROS level in oocytes, reduced the damage caused by oxidative stress in oocytes, and promoted the recovery of oocyte quality. This finding is consistent with the increase in ROS levels induced by E2 through ER β in human seminoma cell lines⁷². The proportion of MII eggs with chromosome arrangement and abnormal spindle morphology was greater in older women (40-45 years) than in younger women (20-25 years) (79% vs. 27%)⁷³. This finding suggested that spindle assembly may be abnormal when oocytes age and when their quality decreases. In this study, we found that

the inhibition of high ER β expression may be related to the recovery of spindle formation, suggesting that PHTPP can also promote the improvement of MII egg quality by improving the spindle assembly process.

Both an increase in ROS levels and abnormal spindle assembly can cause a decrease in oocyte quality and a decrease in developmental potential. Therefore, under the premise that sperm quality was normal, and the fertilization environment was consistent between the different groups, the 2-cell embryo and blastocyst formation rates of the Cy group decreased, suggesting the poor potential of oocytes to develop into embryos and the decreased quality of embryos in the Cy group. After the application of PHTPP, the proportion of 2-cell embryos and blastocysts increased. These findings suggested that PHTPP can improve the quality of oocytes, restore their developmental potential, and improve embryonic development in mice with DOR. Moreover, the litter size of mice with DOR increased following natural mating, suggesting that the fertility of mice with DOR also improved after PHTPP administration.

There are still many limitations in this study. Although many studies have confirmed its feasibility, the toxicity of chemical drugs itself does not rule out an effect on oocytes and granulosa cells in the ovary, which may not be able to truly simulate DOR in the population not receiving chemotherapy. In addition, in the present study, we investigated the effect of PHTPP treatment on the quality of granulosa cells and oocytes, but whether the effect on oocytes is caused by direct or indirect effects through gap junctions remains to be further explored. ER β was the core factor identified in this study, and how its isoforms play a role in DOR is also worth exploring.

Here, we elucidated the molecular mechanism by which ER β induces ovarian GC apoptosis through the FOXO3a/autophagy pathway and confirmed the protective effect of the ER β antagonist PHTPP on ovarian reserve and fertility *in vivo*. These results suggest that PHTPP may be a promising medication for treating DOR in a clinical setting. In the future, an ovary-specific ER β gene knockout mouse model needs to be constructed to obtain more direct and reliable evidence.

Author contributions

Fangyuan Li, Jingwen Zhu and Jinchen Liu performed the experiments. Jingwen Zhu and Peili Wu designed the research. Yongyan Hu assisted in oocyte retrieval and IVF-ET in mice. Cheng Zeng, Ruihui Lu and Ning Wu performed the analysis and provided constructive discussions. Qing Xue developed the idea for the study and revised the manuscript.

Acknowledgements

The authors thank Professor Lei Zhang for her assistance in the electron microscopy experiments. This study was supported by a grant from the National Natural Science Foundation of China Major Research Program Cultivation Project (91949113).

Conflict of interest

The authors declare no potential conflicts of interest with respect to the research, authorship, and/or publication of this article.

Supplementary Materials

The Supplementary data can be found online at: www.aginganddisease.org/EN/10.14336/AD.2024.0221.

References

- [1] Zhang QL, Lei YL, Deng Y, Ma RL, Ding XS, Xue W, et al. (2023). Treatment Progress in Diminished Ovarian Reserve: Western and Chinese Medicine. *Chin J Integr Med*, 29: 361.
- [2] Liang C, Zhang X, Qi C, Hu H, Zhang Q, Zhu X, et al. (2021). UHPLC-MS-MS analysis of oxylipins metabolomics components of follicular fluid in infertile individuals with diminished ovarian reserve. *Reprod Biol Endocrinol*, 19: 143.
- [3] Mutlu MF, Erdem A (2012). Evaluation of ovarian reserve in infertile patients. *J Turk Ger Gynecol Assoc*, 13: 196.
- [4] Tu X, You B, Jing M, Lin C, Zhang R (2021). Progestin-Primed Ovarian Stimulation Versus Mild Stimulation Protocol in Advanced Age Women with Diminished Ovarian Reserve Undergoing Their First In Vitro Fertilization Cycle: A Retrospective Cohort Study. *Front Endocrinol (Lausanne)*, 12: 801026.
- [5] Richardson MC, Guo M, Fauser BC, Macklon NS (2014). Environmental and developmental origins of ovarian reserve. *Hum Reprod Update*, 20: 353.
- [6] Alam MH, Miyano T (2020). Interaction between growing oocytes and granulosa cells in vitro. *Reprod Med Biol*, 19: 13.
- [7] Sun Z, Zhang H, Wang X, Wang QC, Zhang C, Wang JQ, et al. (2018). TMCO1 is essential for ovarian follicle development by regulating ER Ca (2+) store of granulosa cells. *Cell Death Differ*, 25: 1686.
- [8] Yeung CK, Wang G, Yao Y, Liang J, Tenny Chung CY, Chuai M, et al (2017). BRE modulates granulosa cell death to affect ovarian follicle development and atresia in the mouse. *Cell Death Dis*, 8: e2697.
- [9] Matsuda F, Inoue N, Manabe N, Ohkura S (2012). Follicular growth and atresia in mammalian ovaries: regulation by survival and death of granulosa cells. *J Reprod Dev*, 58: 44.
- [10] Fan Y, Chang Y, Wei L, Chen J, Li J, Goldsmith S, et al (2019). Apoptosis of mural granulosa cells is increased in women with diminished ovarian reserve. *J Assist Reprod Genet*, 36: 1225.
- [11] Liu W, Chen M, Liu C, Wang L, Wei H, Zhang R, et al (2023). Epg5 deficiency leads to primary ovarian insufficiency due to WT1 accumulation in mouse granulosa cells. *Autophagy*, 19: 644.
- [12] Levine B, Kroemer G (2019). Biological Functions of Autophagy Genes: A Disease Perspective. *Cell*, 176: 11.
- [13] Zhu M, Miao S, Zhou W, Elnesr SS, Dong X, Zou X (2021). MAPK, AKT/FoxO3a and mTOR pathways are involved in cadmium regulating the cell cycle, proliferation and apoptosis of chicken follicular granulosa cells. *Ecotoxicol Environ Saf*, 214: 112091.
- [14] Choi JY, Jo MW, Lee EY, Yoon BK, Choi DS (2010). The role of autophagy in follicular development and atresia in rat granulosa cells. *Fertil Steril*, 93: 2532.
- [15] Choi J, Jo M, Lee E, Choi D (2011). Induction of apoptotic cell death via accumulation of autophagosomes in rat granulosa cells. *Fertil Steril*, 95: 1482.
- [16] Choi J, Jo M, Lee E, Choi D (2014). AKT is involved in granulosa cell autophagy regulation via mTOR signaling during rat follicular development and atresia. *Reproduction*, 147: 73.
- [17] Zhang H, Lin F, Zhao J, Wang Z (2020). Expression Regulation and Physiological Role of Transcription Factor FOXO3a During Ovarian Follicular Development. *Front Physiol*, 11: 595086.
- [18] Dusabimana T, Kim SR, Kim HJ, Park SW, Kim H (2019). Nobiletin ameliorates hepatic ischemia and reperfusion injury through the activation of SIRT-1/FOXO3a-mediated autophagy and mitochondrial biogenesis. *Exp Mol Med*, 51: 1.
- [19] Cao DJ, Jiang N, Blagg A, Johnstone JL, Gondalia R, Oh M, et al (2013). Mechanical unloading activates FoxO3 to trigger Bnip3-dependent cardiomyocyte atrophy. *J Am Heart Assoc*, 2: e000016.
- [20] Guo Y, Zhao Y, Zhou Y, Tang X, Li Z, Wang X (2019). LZ-101, a novel derivative of danofloxacin, induces mitochondrial apoptosis by stabilizing FOXO3a via blocking autophagy flux in NSCLC cells. *Cell Death Dis*, 10: 484.
- [21] Wang F, Chen X, Sun B, Ma Y, Niu W, Zhai J, et al. (2021). Hypermethylation-mediated downregulation of lncRNA PVT1 promotes granulosa cell apoptosis in premature ovarian insufficiency via interacting with Foxo3a. *J Cell Physiol*, 236: 5162.
- [22] Matsuda F, Inoue N, Maeda A, Cheng Y, Sai T, Gonda H, et al. (2011). Expression and function of apoptosis initiator FOXO3 in granulosa cells during follicular atresia in pig ovaries. *J Reprod Dev*, 57: 151.
- [23] Richards JS (1980). Maturation of ovarian follicles: actions and interactions of pituitary and ovarian hormones on follicular cell differentiation. *Physiol Rev*, 60: 51.
- [24] Jefferson WN, Couse JF, Banks EP, Korach KS, Newbold RR (2000). Expression of estrogen receptor

- beta is developmentally regulated in reproductive tissues of male and female mice. *Biol Reprod*, 62: 310.
- [25] Drummond AE, Fuller PJ (2010). The importance of ERbeta signalling in the ovary. *J Endocrinol*, 205: 15.
- [26] Guido C, Panza S, Santoro M, Avena P, Panno ML, Perrotta I, et al. (2012). Estrogen receptor beta (ER β) produces autophagy and necroptosis in human seminoma cell line through the binding of the Sp1 on the phosphatase and tensin homolog deleted from chromosome 10 (PTEN) promoter gene. *Cell Cycle*, 11: 2911.
- [27] Su Q, Wu Q, Chen K, Wang J, Sarwar A, Zhang Y (2022). Induction of estrogen receptor β -mediated autophagy sensitizes breast cancer cells to TAD1822-7, a novel biphenyl urea taspine derivative. *Mol Biol Rep*, 49: 1223.
- [28] Song P, Li Y, Dong Y, Liang Y, Qu H, Qi D, et al. (2019). Estrogen receptor β inhibits breast cancer cells migration and invasion through CLDN6-mediated autophagy. *J Exp Clin Cancer Res*, 38: 354.
- [29] Yang ZM, Yang MF, Yu W, Tao HM (2019). Molecular mechanisms of estrogen receptor β -induced apoptosis and autophagy in tumors: implication for treating osteosarcoma. *J Int Med Res*, 47: 4644.
- [30] Dey P, Ström A, Gustafsson J (2014). Estrogen receptor β upregulates FOXO3a and causes induction of apoptosis through PUMA in prostate cancer. *Oncogene*, 33: 4213.
- [31] Klionsky DJ, Abdelmohsen K, Abe A, Abedin MJ, Abeliovich H, Acevedo Arozena A, et al. (2016). Guidelines for the use and interpretation of assays for monitoring autophagy (3rd edition). *Autophagy*, 12: 1.
- [32] Wang XN, Roy SK, Greenwald GS (1991). In vitro DNA synthesis by isolated preantral to preovulatory follicles from the cyclic mouse. *Biol Reprod*, 44: 857.
- [33] Cordts EB, Christofolini DM, Dos Santos AA, Bianco B, Barbosa CP (2011). Genetic aspects of premature ovarian failure: a literature review. *Arch Gynecol Obstet*, 283: 635.
- [34] Xu S, Ma Y, Chen Y, Pan F (2021). Role of Forkhead box O3a transcription factor in autoimmune diseases. *Int Immunopharmacol*, 92: 107338.
- [35] Klein-Hitpass L, Ryffel GU, Heitlinger E, Cato AC (1988). A 13 bp palindrome is a functional estrogen responsive element and interacts specifically with estrogen receptor. *Nucleic Acids Res*, 16: 647.
- [36] Hasson O, Stone L (2009). Male infertility, female fertility and extrapair copulations. *Biol Rev Camb Philos Soc*, 84: 225.
- [37] Guan M, Bogani D, Marschall S, Raspa M, Takeo T, Nakagata N, et al. (2014). In vitro fertilization in mice using the MBCD-GSH protocol. *Curr Protoc Mouse Biol*, 4: 67.
- [38] Liu H, Jiang C, La B, Cao M, Ning S, Zhou J, et al. (2021). Human amnion-derived mesenchymal stem cells improved the reproductive function of age-related diminished ovarian reserve in mice through Ampk/FoxO3a signaling pathway. *Stem Cell Res Ther*, 12: 317.
- [39] Fàbregues F, Ferreri J, Méndez M, Calafell JM, Otero J, Farré R (2020). In Vitro Follicular Activation and Stem Cell Therapy as a Novel Treatment Strategies in Diminished Ovarian Reserve and Primary Ovarian Insufficiency. *Front Endocrinol (Lausanne)*, 11: 617704.
- [40] Tachibana M, Kuno T, Yaegashi N (2018). Mitochondrial replacement therapy and assisted reproductive technology: A paradigm shift toward treatment of genetic diseases in gametes or in early embryos. *Reprod Med Biol*, 17: 421.
- [41] Vargas JNS, Hamasaki M, Kawabata T, Youle RJ, Yoshimori T (2023). The mechanisms and roles of selective autophagy in mammals. *Nat Rev Mol Cell Biol*, 24: 167.
- [42] Zhou J, Peng X, Mei S (2019). Autophagy in Ovarian Follicular Development and Atresia. *Int J Biol Sci*, 15: 726.
- [43] Choi J, Jo M, Lee E, Choi D (2011). The role of autophagy in corpus luteum regression in the rat. *Biol Reprod*, 85: 465.
- [44] O'Connell JM, Pepling ME (2021). Primordial Follicle Formation - Some Assembly Required. *Curr Opin Endocr Metab Res*, 18: 118.
- [45] Havelock JC, Rainey WE, Carr BR (2004). Ovarian granulosa cell lines. *Mol Cell Endocrinol*, 228: 67.
- [46] Haddad YH, Said RS, Kamel R, Morsy EME, El-Demerdash E (2020). Phytoestrogen genistein hinders ovarian oxidative damage and apoptotic cell death-induced by ionizing radiation: co-operative role of ER- β , TGF- β , and FOXL-2. *Sci Rep*, 10: 13551.
- [47] Wang Y, Liu W, Du J, Yu Y, Liang N, Liang M, et al. (2015). NGF promotes mouse granulosa cell proliferation by inhibiting ESR2 mediated down-regulation of CDKN1A. *Mol Cell Endocrinol*, 406: 68.
- [48] Mu X, Tu Z, Chen X, Hong Y, Geng Y, Zhang Y, et al. (2021). In utero Exposure to Excessive Estrogen Impairs Homologous Recombination and Oogenesis via Estrogen Receptor 2 in Mice. *Front Cell Dev Biol*, 9: 669732.
- [49] Chakravarthi VP, Ghosh S, Roby KF, Wolfe MW, Rumi MAK. (2020). A Gatekeeping Role of ESR2 to Maintain the Primordial Follicle Reserve. *Endocrinology*, 161:
- [50] Ruddy SC, Lau R, Cabrita MA, McGregor C, McKay BC, Murphy LC, et al. (2014). Preferential estrogen receptor β ligands reduce Bcl-2 expression in hormone-resistant breast cancer cells to increase autophagy. *Mol Cancer Ther*, 13: 1882.
- [51] Datta J, Willingham N, Manouchehri JM, Schnell P, Sheth M, David JJ, et al. (2022). Activity of Estrogen Receptor β Agonists in Therapy-Resistant Estrogen Receptor-Positive Breast Cancer. *Front Oncol*, 12: 857590.
- [52] Liu H, Luo LL, Qian YS, Fu YC, Sui XX, Geng YJ, et al. (2009). FOXO3a is involved in the apoptosis of naked oocytes and oocytes of primordial follicles from neonatal rat ovaries. *Biochem Biophys Res Commun*, 381: 722.
- [53] Kruse R, Pedersen AJ, Kristensen JM, Petersson SJ, Wojtaszewski JF, Højlund K (2017). Intact initiation of autophagy and mitochondrial fission by acute exercise in skeletal muscle of patients with Type 2 diabetes. *Clin Sci (Lond)*, 131: 37.

- [54] Cai J, Li R, Xu X, Zhang L, Lian R, Fang L, et al. (2018). CK1 α suppresses lung tumour growth by stabilizing PTEN and inducing autophagy. *Nat Cell Biol*, 20: 465.
- [55] Ma R, Karthik GM, Lötvot J, Haglund F, Rosin G, Katchy A, et al. (2017). Estrogen Receptor β as a Therapeutic Target in Breast Cancer Stem Cells. *J Natl Cancer Inst*, 109: 1.
- [56] Han SJ, Jung SY, Wu SP, Hawkins SM, Park MJ, Kyo S, et al. (2015). Estrogen Receptor β Modulates Apoptosis Complexes and the Inflammasome to Drive the Pathogenesis of Endometriosis. *Cell*, 163: 960.
- [57] Shao T, Ke H, Liu R, Xu L, Han S, Zhang X, et al. (2022). Autophagy regulates differentiation of ovarian granulosa cells through degradation of WT1. *Autophagy*, 18: 1864.
- [58] Gao W, Liang JX, Ma C, Dong JY, Yan Q (2017). The Protective Effect of N-Acetylcysteine on Ionizing Radiation Induced Ovarian Failure and Loss of Ovarian Reserve in Female Mouse. *Biomed Res Int*, 2017: 4176170.
- [59] Guiraldelli MF, Eyster C, Wilkerson JL, Dresser ME, Pezza RJ (2013). Mouse HFM1/Mer3 is required for crossover formation and complete synapsis of homologous chromosomes during meiosis. *PLoS Genet*, 9: e1003383.
- [60] Zhang Q, Huang Y, Sun J, Gu T, Shao X, Lai D (2019). Immunomodulatory effect of human amniotic epithelial cells on restoration of ovarian function in mice with autoimmune ovarian disease. *Acta Biochim Biophys Sin (Shanghai)*, 51: 845.
- [61] Kalich-Philosoph L, Roness H, Carmely A, Fishel-Bartal M, Ligumsky H, Paglin S, et al. (2013). Cyclophosphamide triggers follicle activation and "burnout"; AS101 prevents follicle loss and preserves fertility. *Sci Transl Med*, 5: 185ra62.
- [62] Meiorow D, Biederman H, Anderson RA, Wallace WH (2010). Toxicity of chemotherapy and radiation on female reproduction. *Clin Obstet Gynecol*, 53: 727.
- [63] Spears N, Lopes F, Stefansdottir A, Rossi V, De Felici M, Anderson RA, et al. (2019). Ovarian damage from chemotherapy and current approaches to its protection. *Hum Reprod Update*, 25: 673.
- [64] Qin X, Zhao Y, Zhang T, Yin C, Qiao J, Guo W, et al. (2022). TrkB agonist antibody ameliorates fertility deficits in aged and cyclophosphamide-induced premature ovarian failure model mice. *Nat Commun*, 13: 914.
- [65] Han X, Bai L, Wang Y, Li Y, Zhao D, Hu G, et al. (2020). Ovarian Index of KM Mice Influenced by Longer Term Consumption of Microwave-Heated Milk. *J Food Prot*, 83: 1066.
- [66] Koike M, Kanda A, Kido K, Goto K, Kumasako Y, Nagaki M, et al. (2018). Effects of cyclophosphamide administration on the in vitro fertilization of mice. *Reprod Med Biol*, 17: 262.
- [67] Bines J, Oleske DM, Cobleigh MA (1996). Ovarian function in premenopausal women treated with adjuvant chemotherapy for breast cancer. *J Clin Oncol*, 14: 1718.
- [68] Seifer DB, Baker VL, Leader B (2011). Age-specific serum anti-Müllerian hormone values for 17,120 women presenting to fertility centers within the United States. *Fertil Steril*, 95: 747.
- [69] Meiorow D, Lewis H, Nugent D, Epstein M (1999). Subclinical depletion of primordial follicular reserve in mice treated with cyclophosphamide: clinical importance and proposed accurate investigative tool. *Hum Reprod*, 14: 1903.
- [70] Pascuali N, Scotti L, Di Pietro M, Oubiña G, Bas D, May M, et al. (2018). Ceramide-1-phosphate has protective properties against cyclophosphamide-induced ovarian damage in a mice model of premature ovarian failure. *Hum Reprod*, 33: 844.
- [71] Meiorow D, Epstein M, Lewis H, Nugent D, Gosden RG (2001). Administration of cyclophosphamide at different stages of follicular maturation in mice: effects on reproductive performance and fetal malformations. *Hum Reprod*, 16: 6.
- [72] Panza S, Santoro M, De Amicis F, Morelli C, Passarelli V, D'Aquila P, et al. (2017). Estradiol via estrogen receptor beta influences ROS levels through the transcriptional regulation of SIRT3 in human seminoma Tcam-2 cells. *Tumour Biol*, 39: 1010428317701642.
- [73] Battaglia DE, Goodwin P, Klein NA, Soules MR (1996). Influence of maternal age on meiotic spindle assembly in oocytes from naturally cycling women. *Hum Reprod*, 11: 2217.